

## Modification of an epoxy resin with a fluoroepoxy oligomer for improved mechanical and tribological properties

Witold Brostow<sup>a,\*</sup>, Wunpen Chonkaew<sup>a,b</sup>, Kevin P. Menard<sup>a,c</sup>, Thomas W. Scharf<sup>d</sup>

<sup>a</sup> Laboratory of Advanced Polymers & Optimized Materials (LAPOM), Department of Materials Science and Engineering, College of Engineering, University of North Texas, Denton, TX 76203-5310, United States

<sup>b</sup> Department of Chemistry, Faculty of Science, King Mongkut's University of Technology Thonburi, 126 Prach-utis Road, Bangmod, Toong-kru, Bangkok 10140, Thailand

<sup>c</sup> Perkin Elmer & Life Science, Shelton, CT 06484-4794, United States

<sup>d</sup> Department of Materials Science and Engineering, College of Engineering, University of North Texas, Denton, TX 76203-5310, United States

### ARTICLE INFO

#### Article history:

Received 3 September 2008

Received in revised form 3 December 2008

Accepted 4 December 2008

#### Keywords:

Friction

Wear

Storage modulus

Epoxy

Polymer tribology

### ABSTRACT

A commercial diglycidylether of bisphenol-A (DGEBA) epoxy was modified by blending with a fluoroepoxy oligomer diglycidyl of trifluoromethyl aniline (DGTF), with the content of DGTF 2.5–20 phr. Thermogravimetry shows that the incorporation of tertiary amines results in a reduction in thermal stability. The storage modulus in the glassy state increases significantly as a function of DGTF content due to antiplasticization. Higher wear resistance and lower dynamic friction are achieved by incorporation of DGTF. At least for the range of this study, while increasing the amount of DGTF, both wear rate and dynamic friction are reduced due to the formation of a protective transfer film (third body). The product of flexural strength and strain at deflection point is found to correlate with the reduction in wear rate.

© 2008 Elsevier B.V. All rights reserved.

### 1. Introduction

One useful method to improve performance of epoxy resins is chemical modification with fluorine functional groups. Due to the presence of fluorine atoms [1–3], compounds develop outstanding properties: chemical and thermal stability, weathering resistance, low dielectric constant [4], low surface tension, low friction, hydrophobicity and oleophobicity. Thus, the introduction of fluorine atoms into the systems may combine those properties of fluorinated compounds and the advantages of epoxy resins. The fluorinated compounds, acting as solid lubricants, are added to a polymer to decrease adhesion or form a protective transfer film with a low interfacial shear stress between the rubbing counterbodies, thus reducing the friction and wear rate (tribological properties) of the polymer matrix. We recall analysis of effects of third bodies on wear of polymer surfaces by Briscoe, Tabor and coworkers [5–7]. Effects of surface and interfacial tension on properties have been recently reviewed by Kopczynska and Ehrenstein [8].

Literature on mechanical properties of polymer-based materials (PBMs) is very extensive—with obvious consequences for our

understanding of polymer mechanics. By contrast, polymer tribology is understood much less even though the area is not new [9].

This while Rabinowicz [10] convincingly argues how important mitigating wear is for the economic health of any industrial enterprise. Progress in polymer tribology is both experimental [11–13] and computational [14,15]. Among others, this group has demonstrated [16] that the penetration (instantaneous) depth  $R_p$  in sliding wear (multiple scratching along the same groove) is related to  $\tan \delta$  determined in dynamic mechanical testing (DMA, see [17]). Glass transition temperatures have been related to nanoindentation creep [18]; the creep is the slowest at and near the glass transition. Groove profiles perpendicular to the indenter movement direction have been investigated [19]; a relation between the Vickers hardness and the total cross-section area of material displaced by the indenter has been found. Closer to the subject of the present paper, addition of 50 nm diameter silica particles to an epoxy reduces wear (and is also visible in narrower wear tracks) [20]. However, much remains to be done. In this situation the present work is aimed at fluorination of a commercial epoxy and evaluation of consequences of fluorination on tribological properties.

Previous work on the synthesis of fluorinated epoxy monomers and oligomers has been reported. Park et al. synthesized new fluorine-containing epoxy resins by incorporating a phenyl-trifluoromethyl ( $-\text{Ph}-\text{CF}_3$ ) group both into the main chains [4] and into the side chain [2] of epoxy resins. Montefusco et al. [21] synthesized new difunctional fluoro-epoxide monomers, starting by

\* Corresponding author. Fax: +1 940 565 4824.

E-mail address: [wbrostow@yahoo.com](mailto:wbrostow@yahoo.com) (W. Brostow).

URL: <http://www.unt.edu/LAPOM/> (W. Brostow).

allylation of the fluorinated diols and followed by an epoxidation reaction. The monomers obtained showed a higher reactivity with respect to hexanedioldiglycidyl ether (HDGE) when used in UV curing. This behavior was attributed to lower nucleophilicity of glycidyl oxygen in the fluorinated monomers. Surface properties of the cured films were highly hydrophobic even after blending with HDGE. The blend surface exposed to air had similar hydrophobicity as pure fluoroepoxy cured films. Such high hydrophobicity implies a selective enrichment of the fluorinated segments at the air surface. Sangermano et al. [22] have shown in photocured systems of 1,4-cyclohexanedimethanol-diglycidyl ether a selective migration of F atoms to the air surface of UV cured films. Small amounts of two epoxy-fluorinated monomers, 3-(perfluorooctyl)-1,2-propenoxide and 3-(1H, 1H, 9H-hexadecafluorononyloxy)-1,2-propenoxide, were used as modifying additives. Surface properties of UV cured films filled with fluorinated additives at the air surface became highly hydrophobic—while at the mold surface they were unchanged [22]. On the other hand, changes in bulk properties and in kinetics of photopolymerization were not found, apparently due to low amounts of fluorinated additives.

Bilyeu [23] used a fluorinated aromatic amine mixed with a standard aliphatic amine as a curing agent for a commercial diglycidylether of bisphenol-A (DGEBA) epoxy. The resulting cured networks were determined to have lower wear than the unmodified epoxy resins.

van de Grampel et al. [3] proposed other options: the curing agents rather than epoxy monomers were modified. Partially fluorinated diamine monomers were prepared by reaction of perfluoroalkyl epoxide with a known excess of diamine. The fluorinated epoxy films obtained were stable, and the surface modification was permanent.

An explanation for the improvement in surface properties is the segregation of fluorinated species at the epoxy surface—advantageous in the case of self-stratifying coatings [24–37]. Only a small quantity of fluorinated species, which are needed to produce the surface with low interfacial energy, migrates to the surface of the bulk to form a coating [3,38].

Blending is an alternative method. Uses of nonreactive fluoropolymers as the epoxy modifiers that blend with a commercial epoxy have been proposed [3,35–38]. Kasemura et al. [39] blended fluorine-containing block copolymers, consisting of methylacrylate, glycidyl methylacrylate and 3, 3, 4, 4, 5, 5, 6, 6, 7, 7, 8, 8, 9, 9, 10, 10, 10-heptadecafluorodecyl acrylate with an epoxy resin. There was improvement of water repellency. The fluorocarbon segments with low surface energy tended towards the surface, providing there a higher concentration of F atoms.

We have used earlier [35–38] a fluorinated poly(aryl ether ketone) as a modifier for diglycidyl ether of bisphenol-A epoxy system. Curing was performed at 24 and 70 °C. There was a significant lowering in both static and dynamic friction at 5 wt.% of the additive for the systems cured at 24 °C, while for those cured at 70 °C the friction increased. There was also a decrease in scratch depths. According to phase contrast in the scanning electron microscope (SEM) there was a phase inversion at the surface, with the fluoropolymer forming a continuous phase for curing at 24 °C, but not at 70 °C. The improvement of tribological properties at 24 °C was due to that continuous fluoropolymer phase.

Fluorination of polymer surfaces by an implantation is another option leading to hydrophobic surfaces. du Toit et al. [40] obtained a marked decrease in the total surface tension of high-density polyethylene (HDPE) by direct fluorination with fluorine gas. To improve water repellency of polymer surfaces, highly fluorinated compounds such as CF<sub>4</sub>, C<sub>2</sub>F<sub>6</sub> and SF<sub>6</sub> [41–44] have been used as plasma gases in the implantation of fluorine functionalities on polymer surfaces. Physical methods have also been applied. Thus, Han et al. [45] enhanced surface hydrophobicity of epoxy resins by curing

them against polytetrafluoroethylene (PTFE) mold. PTFE molecules anchored firmly on the epoxy surface—a stable fluorination. The fluorinated epoxy resin surfaces were as highly hydrophobic as the pristine PTFE surface.

In this study, a new fluoro-functionalized epoxy oligomer was synthesized and blended with the commercial DGEBA epoxy resin. The effects of fluoro-functionalized epoxy oligomer content on the thermal, mechanical and tribological properties were investigated and the respective mechanisms discussed.

## 2. Experimental

### 2.1. Materials

Diglycidyl ether of bisphenol-A (DGEBA) and aliphatic polyamines (Hardener 1) from System Three were used as a commercial epoxy resin and a curing agent, respectively. An epoxide equivalent weight of the commercial epoxy resin is 210 g eq<sup>-1</sup>. The amine hydrogen equivalent weight of the curing agent is 93 g eq<sup>-1</sup>. Epichlorohydrin and *m*-trifluoromethyl aniline were purchased from Aldrich. All chemicals were used without further purification. Diglycidyl of trifluoromethyl aniline (DGTF) epoxy oligomer was synthesized as described below.

### 2.2. Synthesis of diglycidyl of trifluoromethyl aniline (DGTF) epoxy oligomer

Trifluoromethyl aniline (20.0 g) and trace of water were charged in a four-neck round-bottom flask equipped with a mechanical stirrer, reflux condenser, dropping funnel and thermometer controller. The mixture was heated to 60–65 °C and epichlorohydrin (57.4 g) was added dropwise over 1.5 h at the same temperature with agitation. After a 3-h holding period, the temperature was lowered to 50–55 °C and 50% aq. NaOH solution was introduced dropwise during 1 h. The mixture was heated again to 60–65 °C and held further for 30 min. The mixture was then cooled to room temperature and neutralized with 50% acetic acid, and allowed to separate into layers. The organic phase was separated and treated with warm water (about 60 °C) until the by-product salt was completely removed; the organic phase was then dried over sodium sulfate. The obtained product was purified in a vacuum oven at 70–90 °C and 100–150 Torr.

### 2.3. Determination of epoxy equivalent weight

The epoxy content of resins is frequently expressed as epoxide equivalent weight (EEW). Epoxy functionalities were determined according to the pyridine/HCl method: hydrochlorination reaction of epoxy, which forms the corresponding chlorohydrins. The residual HCl was then determined by titration with a basic solution. The hydrochlorination reagent, a 0.2 N solution of HCl in pyridine, was prepared by pipetting 17 mL of concentrated hydrochloric acid into 1 L of pyridine and mixing thoroughly. Then 25 mL of the pyridine hydrochlorination reagent were pipetted into a 250 mL round bottle flask, equipped with a standard taper joint. A known amount of sample was added and dissolved by heating the mixture to ≈40 °C. After the dissolution was complete, the mixture was refluxed for 20 min. The flask and contents were cooled. Then 6 mL of distilled water together with 0.2 mL of phenolphthalein indicator solution was added. The titration was made with standard 0.1 M ethanolic potassium hydroxide solution to a definite pink color.

### 2.4. Preparation of DGEBA + DGTF epoxy resins

DGTF was blended with DGEBA at various ratios from 0 phr (part per hundred) to 20.0 phr. The products obtained were then

mixed with stoichiometric amount of polyamine curing agent. The mixtures were poured into silicone open molds and cured at 25 °C for 24 h in an oven under N<sub>2</sub> atmosphere. The cured epoxies were taken off the molds. All samples were stored for at least a week before testing.

### 2.5. Determination of gel content

The gel content or insoluble fraction produced by crosslinking was determined by measuring the weight loss after extracting with chloroform at room temperature for 24 h, according to the ASTM D 2765-95 standard with test method C. The percent extraction was calculated as follows:

$$\% \text{Extraction} = \left[ \frac{(W_o - W_d)}{W_o} \right] \times 100 \quad (1)$$

where  $W_o$  is the original polymer weight and  $W_d$  is the weight of dried gel.

### 2.6. Fourier transform infrared spectroscopy (FTIR)

FTIR was performed with an IR machine from Perkin Elmer. To prepare a liquid film, small amounts of viscous liquid sample were dropped on a KBr infrared plate, which was then mounted to a cell holder. Tests were run under N<sub>2</sub> gas atmosphere.

### 2.7. Thermogravimetric analysis (TGA)

Thermal stability of samples was determined using Pyris 1 TGA from Perkin Elmer. Cured samples were studied at the heating rate of 40 °C/min from 30 to 700 °C in N<sub>2</sub> atmosphere, then from 700 to 1000 °C in air.

### 2.8. Dynamic mechanical analysis (DMA)

DMA was performed using DMA 7e Perkin Elmer machine in the three point bending configuration. The temperature dependence of the storage modulus  $E'$ , loss modulus  $E''$ , and the loss factor  $\tan \delta$  of each cured sample were determined in temperature scan mode at the constant frequency of 1.0 Hz and the scan rate of 5.0 °C/min. The sample size used was about 6.0 mm × 2.0 mm × 20 mm.

### 2.9. Mechanical properties of DGEBA + DGTEFA epoxy systems

Three point bending experiments were performed also on DMA 7e from Perkin Elmer in stress–strain scan mode of operation. The force applied was from 0 N up to the load of permanent deflection at the rate of 100 mN/min. All tests were performed at 25.0 °C. The sample size was about 6.0 mm × 1.5 mm × 20.0 mm.

### 2.10. Pin on disk tribometer

A Nanovea tribometer from Micro Photonics was used to determine friction and wear rates. The pin used was silicon nitride (Si<sub>3</sub>N<sub>4</sub>) ball with a diameter of 3.2 mm. A test pin was loaded perpendicularly against a rotating disk by applying a dead end load; the pin was mounted on a lever arm via a sample holder. The lever arm was kept in a fixed position by a load cell which measures the frictional force. The normal load applied to the level arm during the test was 5.0 N, equivalent to an initial Hertzian contact radius of 226 μm, maximum and mean contact pressures of 47 MPa and 31 MPa, respectively. The rotation speed of the disc was 200 rpm and the radius of wear track was 2.0 mm—what is equivalent to a linear sliding speed of 42 mm/s. The test was performed for 5000 revolutions under ambient conditions (at 22 °C and RH of 35–45%). Friction  $\mu$  values were calculated using Amonton's first

law of friction, namely the resistance to movement caused by friction is proportional to the load [8,46]. The results reported below are averages from 3 to 5 runs based on data points in the steady state regime and thus represent dynamic friction.

### 2.11. Profilometer

Cross-sectional wear track areas after each pin-on-disc friction test were determined with a Veeco Dektak 150 Profilometer. A stylus with tip radius of 12.5 mm was used. The force applied to sample was 2.0 mg and the scan rate was 26.7 mm/s. The instrument amplifies and records a vertical motion of a stylus displaced at a constant speed by the surface to be measured [46].

All samples were cleaned by high pressure air to eliminate all debris before each test. At least 5 scans were run for each sample, and the average value of the area was used to calculate the wear rate, to be discussed in the next section.

### 2.12. Scanning electron microscope (SEM) and optical microscope

The scanning electron microscope (FEI Quanta E-SEM) was used to observe worn surfaces of samples. All samples were gold coated first. After sliding against each sample surface, the silicon nitride ball was investigated for traces of the transfer film using the optical microscope, Nikon Eclipse ME600.

## 3. Results and discussion

### 3.1. Characterization of fluoro-epoxy oligomer

A yellowish viscous liquid was obtained from the reaction of epichlorohydrin (white powder) with trifluoromethyl aniline (yellow liquid) in a strongly basic medium. The synthesized diglycidyl of trifluoromethyl aniline, that is DGTEFA epoxy oligomer, was characterized for the functional groups by FTIR. Fig. 1 shows an infrared spectrum of the synthesized product. The characteristic absorption bands at 853, 1233 and 1259 cm<sup>-1</sup> show the glycidyl of the epoxide. The characteristic absorption band of CF<sub>3</sub> appears at 1322 cm<sup>-1</sup>. The bands at 1614, 1500 and 1165 cm<sup>-1</sup> are attributed to the aromatic rings. The overtone band pattern in the region from 1700 to 2000 cm<sup>-1</sup> is attributed to 1,3-substituted benzene. Bands at 2956 and 2917 cm<sup>-1</sup> are attributed to C–H stretching from CH<sub>2</sub> and CH, respectively. The OH band appears at 3339 cm<sup>-1</sup>.

Thus, from characteristic peaks discussed above, the synthesized product was roughly proved to be DGTEFA. The chemical reaction of epichlorohydrin (EP) with *m*-trifluoromethyl aniline and the prod-

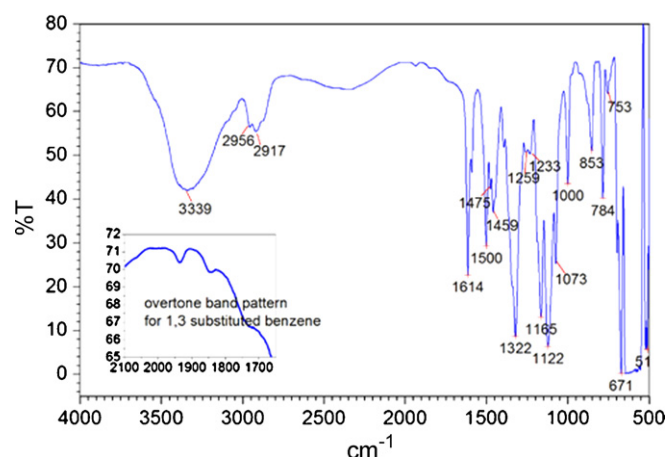
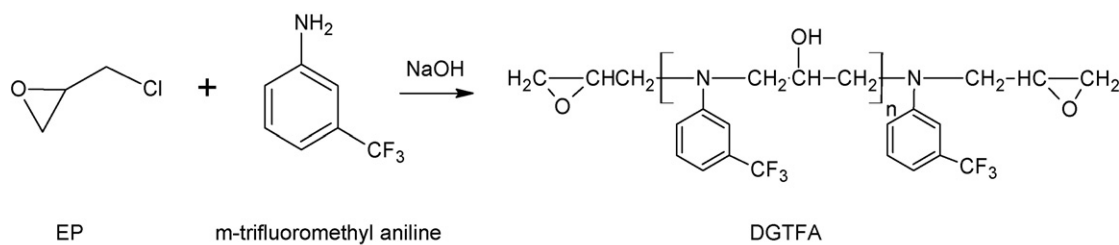


Fig. 1. FTIR spectrum of DGTEFA.



**Scheme 1.** Chemical reaction of epichlorohydrin (EP) with trifluoromethyl aniline.

**Table 1**  
TGA data of the DGEBA + DGTFAs epoxy resins cured with aniline.

DGTFAs content (phr)	IDT (°C)	$T_{max}$ (°C)
0.0	373	396
2.5	365	391
5.0	361	389
10.0	357	382
15.0	351	373
20.0	344	369

uct obtained are shown in Scheme 1. The epoxy content of the product determined in terms of epoxy equivalent weight (EEW) is  $\approx 2000$ . The product was then blended with DGEBA epoxy resin and cured stoichiometrically with polyamines. However, due to a high EEW of the synthesized DGTFAs, the DGEBA + DGTFAs blends only in the concentration range from 2.5 to 20.0 phr of DGTFAs were prepared and studied.

### 3.2. Thermogravimetric analysis (TGA)

Principles of the TGA technique have been described by one of us [47]. We have used TGA to evaluate thermal degradation behavior of cured DGEBA epoxy blended with various amounts of DGTFAs. Thermograms are shown in Fig. 2. The first stage of weight loss represents thermal decomposition of epoxy resins in inert  $N_2$  atmosphere at 200–400 °C. The second stage corresponds to the oxidation of the residuals after switching from  $N_2$  gas to air at 700 °C. We find that the weight loss is shifted to lower temperatures by adding DGTFAs into the DGEBA epoxy resin. The thermal stability parameters, including the initial decomposition temperature (IDT) and the temperature of maximum rate of degradation  $T_{max}$  are listed in Table 1.

We see in Table 1 that both IDT and  $T_{max}$  of the cured epoxy resin decrease when 2.5 phr of DGTFAs is added. These values continue to decrease as the amount of DGTFAs increases. The reason for the

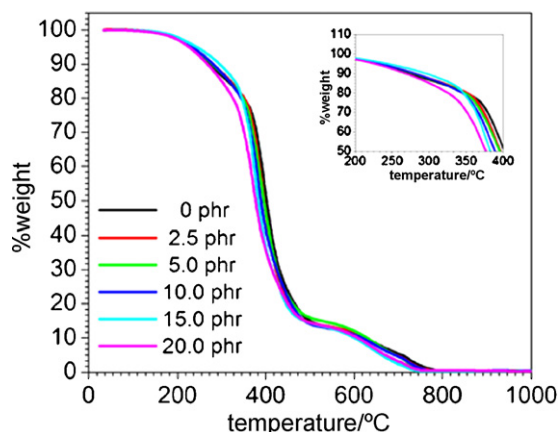


**Fig. 2.** TGA thermograms of cured DGEBA + DGTFAs epoxy resins.

**Table 2**  
DMA results of cured DGEBA + DGTFAs epoxies.

DGTFAs (phr)	$E'$ (Pa) at temperature of			$T_g$ (°C)
	0 °C	25 °C	80 °C	
0.0	$5.54 \times 10^8$	$4.59 \times 10^8$	$8.19 \times 10^6$	55.7
5.0	$6.34 \times 10^8$	$4.47 \times 10^8$	$7.45 \times 10^6$	52.6
10.0	$7.47 \times 10^8$	$4.23 \times 10^8$	$7.92 \times 10^6$	49.3
15.0	$7.89 \times 10^8$	$4.72 \times 10^8$	$7.57 \times 10^6$	48.1
20.0	$9.31 \times 10^8$	$5.56 \times 10^8$	$8.06 \times 10^6$	48.6

decrease in thermal stability is that DGTFAs contains tertiary amine ( $R_3N$ ) functional groups in the molecular backbone. This group can function as a catalyst [48–50] but is less thermally stable than the nitrogen-free multifunctional epoxy resin [50].

### 3.3. Dynamic mechanical analysis (DMA)

Principles of DMA have been described by one of us [17]. Fig. 3 shows the temperature dependence of storage modulus  $E'$ , loss modulus  $E''$  and  $\tan \delta$  for the cured DGEBA blended with DGTFAs samples. The glass transition temperature and the  $E'$  values at three different temperatures are listed in Table 2. The peak of loss modulus  $E''$  is not sharp and symmetrical (Fig. 3b) hence it would be difficult to use them to locate glass transition temperatures  $T_g$ . The  $T_g$  values reported here are those at the maxima value of  $\tan \delta$  ( $T$ ) diagrams.

Fig. 3a shows the storage modulus  $E'$  results. The  $E'$  values at 0 °C, that is in the glassy state, first go up as the amount of DGTFAs increases; then the antiplasticization effect manifests itself. Plasticization, whose main manifestation is the decrease of the glass transition temperature, is generally accompanied by an increase of the glassy modulus in the temperature interval between  $T_\beta$  and  $T_g$  [51]. Here  $T_\beta$  is the first solid state thermophysical transition at a temperature below  $T_g$ . The effect is known as antiplasticization. This phenomenon is common for amine-crosslinked epoxies, and it is usually a consequence of both internal (a change of network structure) and external (incorporation of miscible additives) modification of structure or composition [51].

In Fig. 3c a single relaxation process is observed between  $-20$  °C and  $+100$  °C; it is associated with the glass transition temperature. Only single  $\tan \delta$  peak is found for all compositions; however, the peak widths increase with increasing amounts of DGTFAs. This indicates an increasing degree of inhomogeneity of spatial distribution of crosslink density. A superposition of peaks possibly occurs due to good solubility of DGTFAs oligomers in the epoxy matrix. Thus,  $T_g$  lowering due to the plasticizing effect is observed instead. As seen in Fig. 3 and Table 2,  $T_g$  of the epoxy is reduced by  $\approx 3$  K when 5.0 phr of DGTFAs is introduced.  $T_g$  values keep on decreasing as the amount of DGTFAs increases up to 15.0 phr and then level off. According to the Fox and Loshaek equation [52], it is possible to link the decrease in  $T_g$  to the reduction in the degree of crosslinking as follows:

$$T_{gx} = T_{g\alpha} + \frac{\xi}{M_c} \quad (2)$$

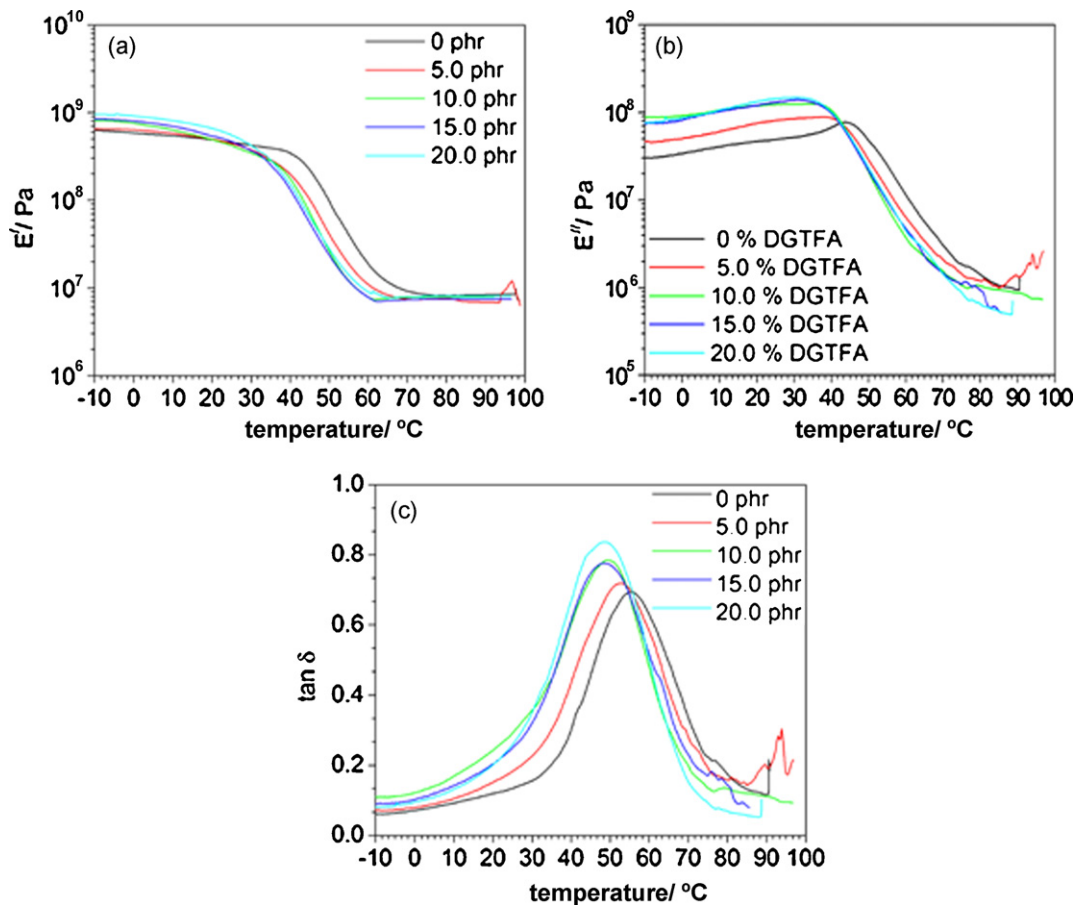


Fig. 3. (a) Storage modulus; (b) loss modulus and (c)  $\tan \delta$  of DGEBA + DGTFAs epoxies cured with polyamine.

where  $T_{gx}$  is the glass transition temperature;  $T_{g\alpha}$  is the glass transition temperature of the linear polymer backbone at infinite molecular weight;  $\zeta$  is a constant dependent on the molecular weight of the unreacted resin and  $M_c$  which defines crosslink density is the molar mass between crosslinks. Another parameter which is used to indicate the crosslink density is the plateau modulus at a given temperature above  $T_g$  [17]. The inverse of storage modulus at rubbery plateau is related to crosslink density. However, we see in Table 2 that plateau storage modulus at 80 °C shows only a slight decrease in the value when DGTFAs oligomer is added. No further significant reduction in the plateau modulus as a function of DGTFAs content is found. To confirm the inference that crosslink density is reduced by adding DGTFAs, percent extraction of the uncrosslinked portion was determined. This value can be used to indicate percent gel or crosslink density of thermosets. The higher the percent extraction, the lower the crosslink density. In Fig. 4, the percent extraction increases about 3.5% when 5.0 phr of DGTFAs is added. Only a small increase in value of percent extraction is observed with increasing amounts of DGTFAs. Nevertheless, this result supports the idea that the addition of DGTFAs causes the reduction in crosslink density.

### 3.4. Mechanical testing results

Fig. 5 shows stress–strain curves from which the flexural modulus and flexural strength at permanent deflection point are determined. Table 3 lists the flexural modulus, percentage strain at permanent deflection point and the flexural strength. The modulus decreases when DGTFAs is added up to 15.0 phr and then levels off  $\approx 20$  phr DGTFAs content. A similar tendency is observed for the

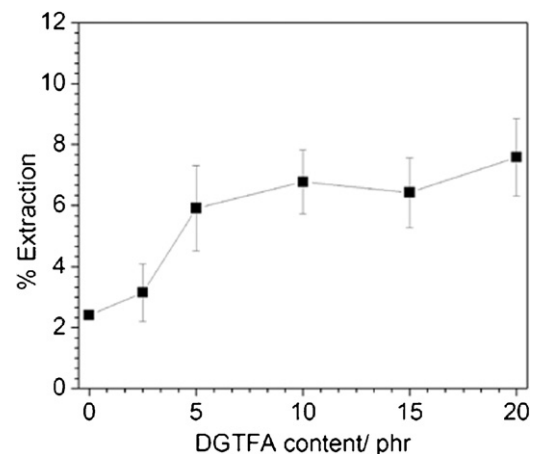


Fig. 4. Percent extraction as a function of DGTFAs content.

storage modulus  $E'$  at 25.0 °C obtained in DMA testing, but only up to 10 phr DGTFAs.  $E'$  then increases with increasing DGTFAs content, and it is even higher than that of the pure epoxy when the addition of DGTFAs is larger than 15.0 phr. This implies that the antiplasticization effect still plays a role at this temperature in DMA testing. The difference in the changes in the modulus as a function of DGTFAs content for these two methods can possibly be explained by the difference in the strain rate to which the materials are exposed. The storage modulus  $E'$  is obtained by applying dynamic force at constant frequency—this, with a low strain response, remains within the linear viscoelastic region. In flexural modulus determination

**Table 3**  
Flexural testing results for DGEBA + DGTFE epoxy resins at 25 °C.

DGTFE content (phr)	Flexural modulus (Pa)	Flexural strength ( $\sigma_f$ ) (MPa)	Strain at deflection point ( $\varepsilon_d$ ) (%)	Product of flexural strength and strain at deflection point ( $\sigma_f \times \varepsilon_d$ )/ $10^{-2}$ MPa
0	$7.21 \times 10^8$	3.52	0.52	1.83
2.5	$7.23 \times 10^8$	7.26	1.03	7.48
5.0	$7.16 \times 10^8$	8.18	1.30	10.63
10.0	$6.27 \times 10^8$	8.00	1.39	11.12
15.0	$4.03 \times 10^8$	7.50	1.90	14.25
20.0	$4.11 \times 10^8$	>12.30 <sup>a</sup>	>3.22 <sup>a</sup>	>39.60 <sup>a</sup>

<sup>a</sup> Specimens were not deformed at the maximum applied load. The flexural stress and strain of materials containing 20.0 phr of DGTFE were collected at 8.0 N, the maximum load allowed to use for DMA 7e.

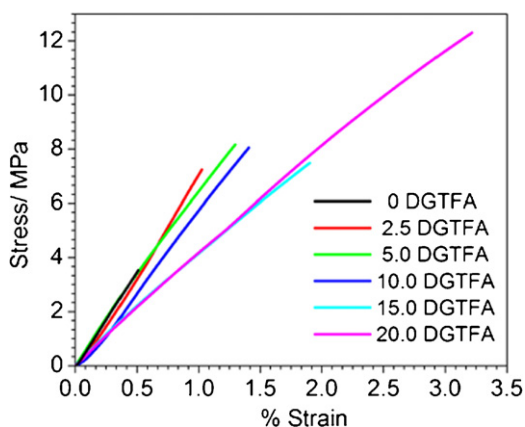


**Fig. 5.** Flexural stress vs. percentage flexural strain for DGEBA+DGTFE resins at 25.0 °C.

when we apply a static force at a constant stress rate getting outside of the elastic region is more likely.

In Table 3 we see how percentage strain at deflection point increases as the amount of DGTFE increases. A lower crosslink density is one possible explanation. The flexural strength increases as the amount of DGTFE increases. This can be advantageous. Toughness is typically determined from the area under the stress–strain curve as the product of the flexural strength  $\sigma_f$  and strain at a deflection point  $\varepsilon_d$ . In Table 3, the toughness of the epoxy resin is improved by adding DGTFE to the epoxy resin. We recall that brittleness of materials is defined in terms of  $E'$  and elongation at break  $\varepsilon_b$  [53,54]. It is plausible to assume that  $\varepsilon_d$  and  $\varepsilon_b$  behave similarly.

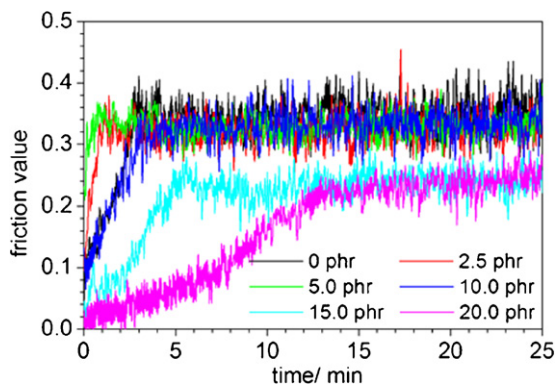


**Fig. 6.** Evolution of friction with time for DGTFE resins blended with various amounts of DGTFE.

**Table 4**  
Surface roughness of DGEBA + DGTFE epoxy resins.

DGTFE content (phr)	$R_a$ (nm)	$R_q$ (nm)
0	519	796
2.5	588	814
5.0	336	467
10.0	146	167
15.0	100	143
20.0	139	164

### 3.5. Friction and wear

Fig. 6 shows evolution of friction of our epoxies in sliding against a silicon nitride ( $\text{Si}_3\text{N}_4$ ) ball. In the case of pure DGEBA epoxy resin, friction remains at an initial value before increasing and attaining a steady state. That increase after a run-in period may be associated with ploughing process because of roughening and/or trapped wear particles which will change the real area of contact and hence the friction. Unlike pure epoxy, the blends with 2.5 and 5.0 phr of DGTFE exhibit steady state values sooner. On the other hand, the 5.0 phr DGTFE resin does not exhibit a run-in period; afterwards the higher the amount of DGTFE, the longer the period is. The run-in phenomenon might be related to the initial formation of ridges [55]. These ridges are progressively worn away until a sufficient amount of wear debris covers the surface leading to a stable lower friction value. Then friction slowly increases to a higher value and levels off at a steady state. Due to smooth surfaces of the blends at high DGTFE content, the increase in friction after the run-in period can be associated with an adhesive component of friction. The smoothing of the surface, due to the sliding of the ball leading to a larger area of contact, contributes to the increasing friction in this regime. We note that surface roughness can be quantified using average

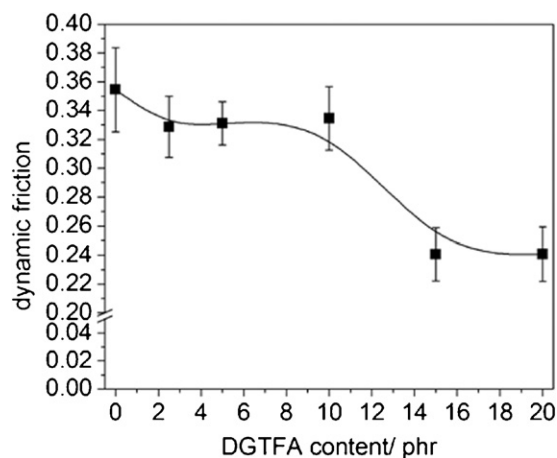


**Fig. 7.** Dynamic (steady state) friction of DGEBA+DGTFE resins as a function of DGTFE content.

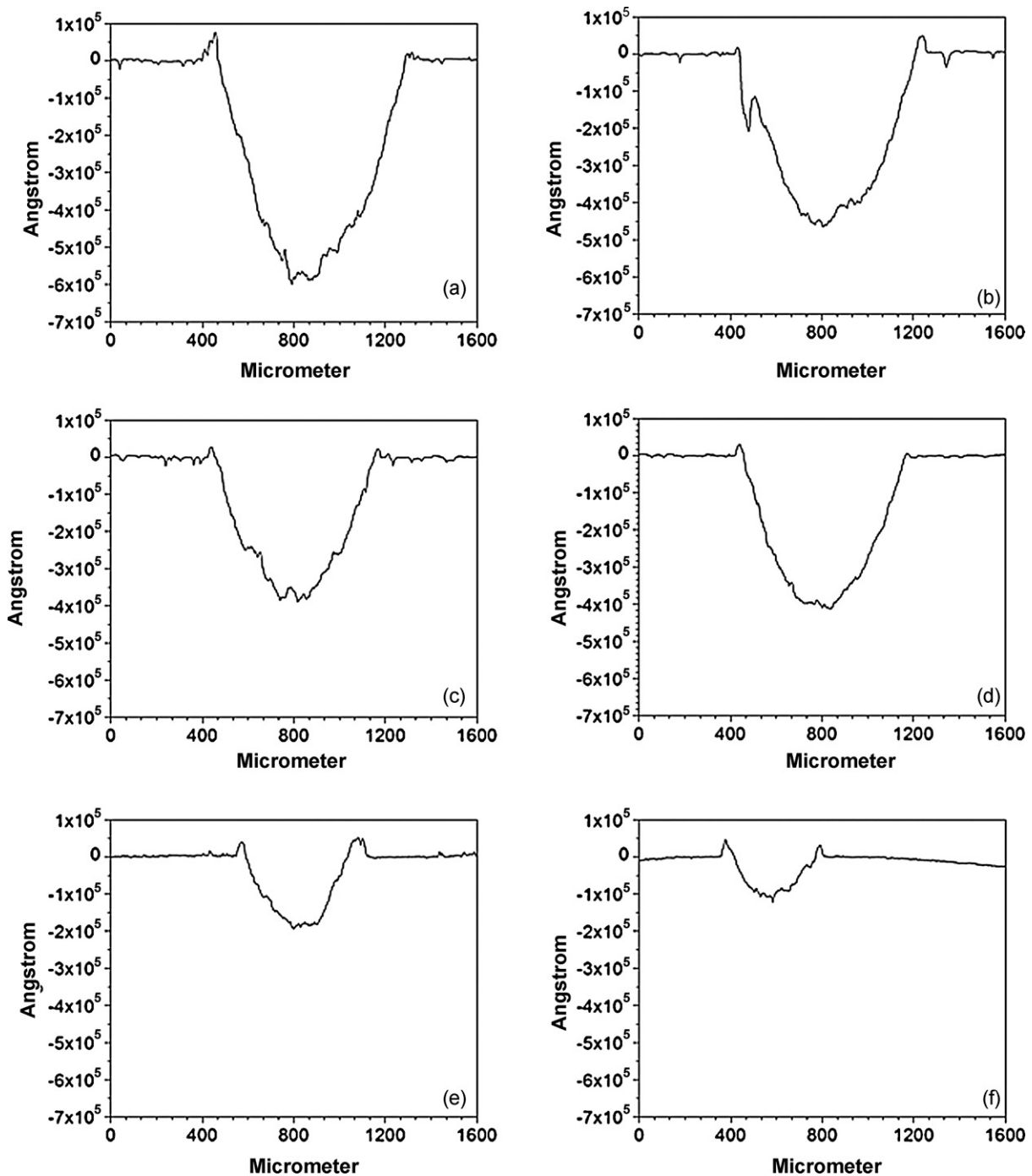


**Fig. 8.** Representative profilometer cross sections of wear traces for: (a) pure DGEBA; DGEBA+; (b) 2.5 phr of DGTFa; (c) +5.0 phr of DGTFa; (d) +10.0 phr of DGTFa; (e) +15.0 phr of DGTFa; and (f) +20.0 phr of DGTFa after sliding against  $\text{Si}_3\text{N}_3$ . Sliding speed: 200 rpm; normal load: 5.0 N; number of revolutions: 5000.

roughness parameters. These parameters usually refer to variations in the height of surface relative to a reference plane. In this study, the center-line average  $R_a$  and the root mean square average ( $R_q$ ) are determined by scanning line profiles with the profilometer. The values are listed in Table 4. Both  $R_a$  and  $R_q$  decrease as the amount of DGTFa increases, indicating that surface roughness of epoxy resin somehow decreases as the amount of DGTFa increases.

To facilitate the comparison, the average values of the dynamic friction (at steady state) are plotted as a function of DGTFa content. We see in Fig. 7 that all blends exhibit lower friction than the pure DGEBA epoxy. Friction decreases slightly when a small

amount (2.5 phr) of DGTFa is added, and it remains approximately constant when 5.0 or 10.0 phr of DGTFa are added. Then at 15.0 DGTFa friction decreases significantly and levels off at 20.0 phr DGTFa.

Worn surfaces of DGEBA epoxy resin and its blends after sliding against a silicon nitride ball are analyzed with the profilometer to quantify wear damage. Fig. 8 shows the cross-section of wear traces on the surfaces. Ridges are observed in all the worn surfaces—formed along the sides of wear traces due to ploughing process. Grooves and peaks left by the material are peeling off—a crack-type process [56].

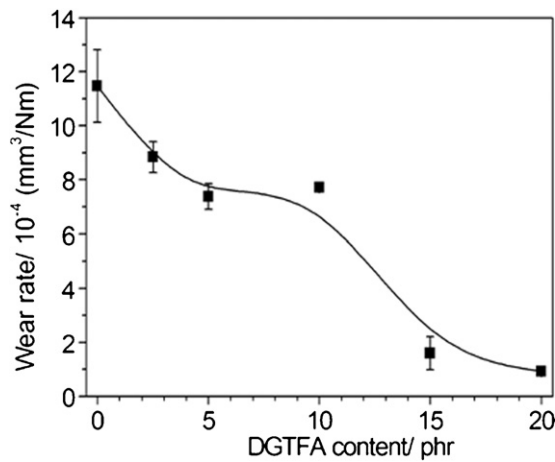


Fig. 9. Wear rate as a function of DGTFa content.

The wear volume  $V_m$  was calculated by multiplying the cross-sectional area obtained from profilometer by the wear trace length as follows:

$$V_m = 2\pi R_m A_m \quad (3)$$

where  $R_m$  and  $A_m$  correspond to the radius of the wear track and to the average cross-section area of the wear track, respectively. To facilitate comparison of the wear resistance of the blends, the wear rate  $K_w$  ( $\text{mm}^3/\text{N m}$ ) was determined as

$$K_w = \frac{V_m}{W_N v t} \quad (4)$$

or

$$K_w = \frac{V_m}{W_N x} \quad (5)$$

where  $W_N$  is the normal load,  $V_m$  is the wear volume,  $v$  is the sliding velocity,  $t$  is the test duration and  $x$  is the sliding distance.

Wear rates of our resins as a function of DGTFa content are shown in Fig. 9. Interestingly, the dependence of wear rate on the DGTFa content is found to be similar to that observed in friction. Wear rate decreases when 2.5 phr of DGTFa is added, and its value seems to remain constant if only 5.0 and 10.0 phr are used. Then with rising DGTFa content, the wear rate exhibits a significant decrease at 15.0 phr, and it levels off again at 20.0 phr. Thus, the incorporation of DGTFa into the system, at least in the range of this study, both improves wear resistance and lowers friction of the epoxy resin. A possible reason for the improvement is that the adhesive component of friction is reduced. According to the adhesive model of friction [57], the interfacial shear stress can be estimated as

$$F_f = \tau A_r \quad (6)$$

By combining Eq. (6) and the Amonton law of friction, one obtains

$$\mu = \frac{F_f}{W_N} = \frac{\tau A_r}{W_N} = \frac{\tau}{p} \quad (7)$$

Then the interfacial shear stress can be determined as

$$\tau = \mu p \quad (8)$$

where  $\mu$  is dynamic friction as before,  $F_f$  the frictional force,  $\tau$  the interfacial shear stress,  $A_r$  is a real contact area,  $W_N$  is the normal force and  $p$  is the average contact pressure. The results are listed in Table 5. The epoxy blended with DGTFa, at high content (15.0 and 20.0 phr), shows a lower interfacial shear stress than the pure epoxy resin – as expected. The incorporation of fluorine functional groups into the systems leads to lower surface energy of epoxy

Table 5

Interfacial shear stress of DGEBA + DGTFa epoxy resins.

DGTFa content (phr)	Interfacial shear stress (MPa)
0	11.0
2.5	10.2
5.0	10.3
10.0	10.4
15.0	7.5
20.0	7.5

[2,3,11,23,35,38]. The fluorine modified epoxy-containing debris is spread over the surface, thereby decreasing the interfacial shear stress; this lowers friction and results in a more gentle wear mechanism.

Due to brittle nature of epoxies, their wear mechanism involves formation of surface and subsurface cracks, conversion from cracks to waves, surface fatigue delamination and formation of debris [58–60]. Conditions applied in the present study ( $1.31 \text{ MPa} \times \text{m/s}$ ) are similar to other studies [59,60] so that surface heating does not affect the wear rate and wear mechanism. However, determination of a sliding interfacial temperature is still necessary. That temperature is estimated [61] as

$$T_{fa} = 0.308 \frac{\mu W_N |U_A - U_B|}{ka} \left( \frac{\chi}{Ua} \right)^{0.5} \quad (9)$$

where  $T_{fa}$  is the average flash temperature in °C,  $U_A$  and  $U_B$  are the surface velocities in m/s of solid A and solid B, respectively,  $U$  is the velocity in m/s of solid A or B,  $a$  is the radius of the contact circle in m,  $\chi$  is the thermal diffusivity in  $\text{m}^2/\text{s}$  and  $k$  is the thermal conductivity in  $\text{W/mK}$ .

When the dynamic (steady state) friction value reaches 0.35, the value of  $T_{fa}$  for pure epoxy is about 40 °C. For the blends the friction values are lower, ranging from 0.33 to 0.24, depending on the amount DGTFa in the epoxy. Thus,  $T_{fa}$  decreases and varies from 38 to 29 °C respectively for our lowest and highest concentrations of DGTFa in epoxy. These values are below the glass transition temperatures for all our systems. The Peclet number

$$Pe = \frac{Ua}{2\chi} \quad (10)$$

representing the heat transfer effect amounts to 47, what indicates a fast moving heat source. The heat generated mostly transfers to the  $\text{Si}_3\text{N}_4$  ball; while ceramics have as a rule lower thermal conductivity than metals,  $\text{Si}_3\text{N}_4$  is known to have relatively high thermal conductivity [62]. Thus, thermal softening due to the frictional heat is not expected.

To further explain the mechanism, the worn surfaces of the epoxy resin and its blends were investigated with SEM. The resins containing 5.0 and 20.0 phr of DGTFa were chosen; see Figs. 7 and 9. Fig. 10 demonstrates a comparison of worn surface of the pure epoxy resin and its blends. The scale-like damage generated under repeated loading is observed, indicating the occurrence of surface fatigue delamination process as shown previously in [60]. The magnified microstructures of the worn surface (Fig. 10b and c) show wear platelets together with chunks of debris loosely smeared on the worn surface. These platelets are formed as a result of generation and propagation of surface and subsurface cracks [46,60]. Small sized platelets and debris found on the worn surface reflect the brittle nature of the epoxy resin. When DGTFa is added (see Fig. 10e and f), larger platelets with more homogeneity are observed. Moreover, platelets seem to adhere more tightly to the worn surface than those found in the pure DGEBA epoxy resin. A further increase in DGTFa content to 20.0 phr (see Fig. 10h and i) results in more continuous and tenacious platelets which become a protective layer of the material underneath. No sign of small sized platelets or debris is found on the worn surface. These results imply that the toughness

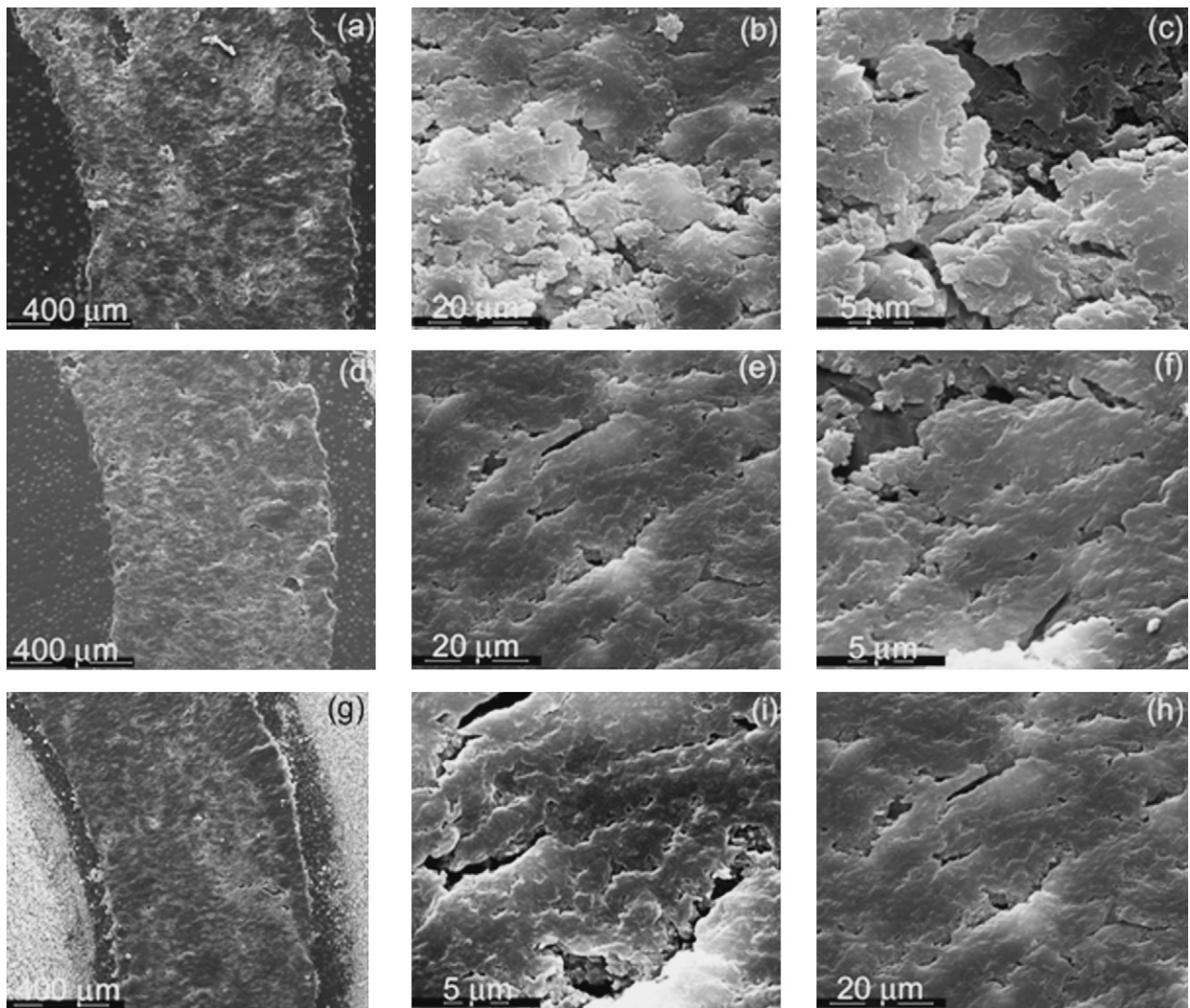


**Fig. 10.** SEM micrographs of the worn surface for (a, b and c) pure DGEBA epoxy resin (d, e and f) DGEBA epoxy blended with 5.0 phr of DGTFAs and (g, h and i) DGEBA epoxy blended with 20.0 phr of DGTFAs. Condition of sliding wear tests: normal load of 5.0 N; sliding speed of 200 rpm, results for 5000 turns. Magnification: 120 $\times$  for (a, d and g), 2000 $\times$  for (b, e and h) and 5000 $\times$  for (c, f and i).

increases when DGTFAs is introduced to the epoxy system; more work is needed to create the same amount of wear. Thus, the higher amount of DGTFAs that is in the system, the lower the wear rate. The protective layer formed at high DGTFAs content is assumed to contribute to significant reduction in wear rate found in the blend with 20.0 phr of DGTFAs.

From the mechanism proposed above, a correlation between the mechanical properties and wear resistance seems to exist. According to Ratner-Lancaster [61,63], wear of polymer is inversely proportional to the product of the fracture stress and fracture strain, representing work needed for tensile fracture, a measure of material toughness. The plot of wear rate as a function of a product of the flexural strength and %strain at a deflection point of DGEBA + DGTFAs epoxy resins is shown in Fig. 11.

It is well known that the phenomenon of material transfer during sliding is important because protective third bodies are formed, e.g. transfer film formation [5–7,64]. The transfer film affects both the friction and wear behavior of materials by several mechanisms: isolates the two “first bodies” from contact (minimizes their wear), controls the friction values (usually through interfacial sliding between the transfer film and wear track), affects the wear rate and wear life (lowers wear by reducing the frictional stresses),

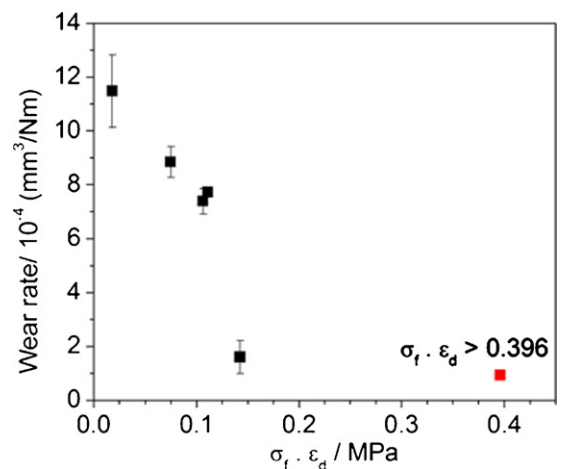


**Fig. 11.** Wear rate as a function of the product of flexural strength and strain at deflection point for DGEBA + DGTFAs epoxy resins. The red point corresponds to the wear rate and  $\sigma_f \cdot \epsilon_d$  of the epoxy with 20 phr DGTFAs. (For interpretation of the references to color in this figure legend, the reader is referred to the web version of the article.)

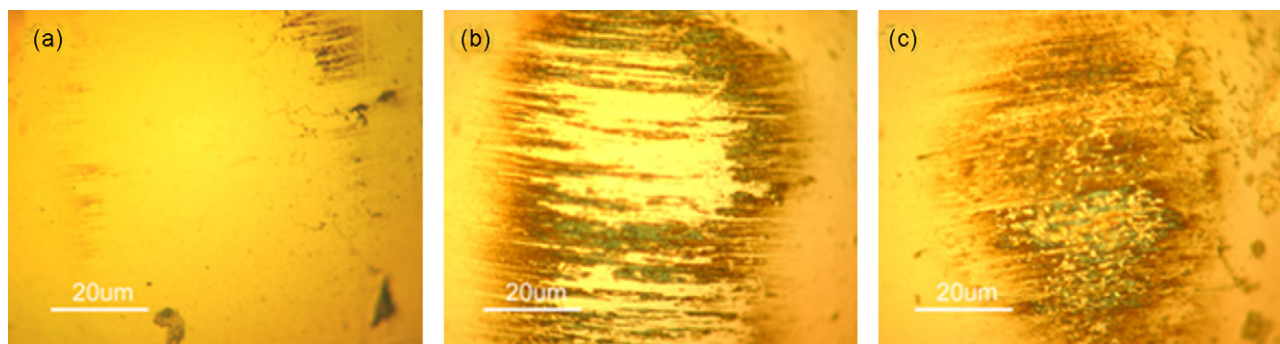


**Fig. 12.** Optical image (200 $\times$ ) of transfer film formed on the surface of  $\text{Si}_3\text{N}_4$  counterface after sliding against (a) pure DGEBA epoxy; (b) DGEBA epoxy blended with 5.0 phr DGTFA; and (c) for 20.0 phr of DGTFA. Normal load: 5.0 N; sliding speed: 200 rpm; 5000 turns.

increases the endurance (third bodies recirculate in and out of the sliding contact). In our case the formation of transfer films is not associated in a significant way with frictional heat generated at contact surfaces during sliding. As already noted,  $T_{fa}$  remains low and thus the effect of frictional heat is minimal.

To investigate transfer film, silicon nitride balls were examined using an optical microscope after sliding against epoxy samples. For pure DGEBA epoxy resin (Fig. 12a), no transfer film is observed; only loose debris is formed with no tendency to adhere to the silicon nitride counterface, also shown in [60]. This result is expected due to the crosslinked structure of the epoxy. However, the addition of DGTFA into the system leads to formation of a transfer film on the  $\text{Si}_3\text{N}_4$  counterface. One possible reason is that the decrease in crosslink density due to the addition of DGTFA enhances the deformation. Enhancement of deformation of the epoxy whose  $T_g$  is low leads to more adhesion of the resin to the counterface. Blends with a higher amount of DGTFA show more transfer film on the  $\text{Si}_3\text{N}_4$  counterface. A continuous and tenacious transfer film is formed when 20.0 phr of DGTFA is incorporated (Fig. 12c).

Thus, an increase in toughness of bulk materials together with the formation of transfer film (a stress reducer [64]) contributes to the reduction of friction and wear rate in our system). Given numerous applications of epoxies [65–67], these are significant results.

## References

- [1] C.B. McCloskey, C.M. Yip, J.P. Santerre, *Macromolecules* 35 (2002) 924–933.
- [2] S.-J. Park, F.-L. Jin, L.-S. Shin, *Mater. Sci. Eng. A* 390 (2005) 240–245.
- [3] R.D. van de Grampel, W. Ming, W.J.H. van Gennip, F. van der Velden, J. Laven, J.W. Niemantsverdriet, R. van der Linde, *Polymer* 46 (2005) 10531–10537.
- [4] J.R. Lee, F.L. Jin, S.J. Park, J.M. Park, *Surf. Coat. Technol.* 180–181 (2004) 650–654.
- [5] B.J. Briscoe, D. Tabor, in: D.T. Clark, J. Feast (Eds.), *Polymer Surfaces*, Wiley, New York, 1978, pp. 1–23.
- [6] B.J. Briscoe, S.K. Sinha, *J. Eng. Tribol.* 216 (2002) 401–413.
- [7] B.J. Briscoe, S.K. Sinha, in: G. Stachowiak (Ed.), *Wear – Materials, Mechanism and Practice*, Wiley, Chichester, 2005, pp. 223–267.
- [8] A. Kopczyńska, G.W. Ehrenstein, *J. Mater. Ed.* 29 (2007) 325–340.
- [9] R.P. Steijn, in: W. Brostow, R.D. Corneliussen (Eds.), *Failure of Plastics*, Hanser, New York, 1986, pp. 356–392.
- [10] E. Rabinowicz, *Friction and Wear of Materials*, second ed., Wiley, New York, 1995.
- [11] W. Brostow, J.-L. Deborde, M. Jaklewicz, P. Olszynski, *J. Mater. Ed.* 25 (2003) 119–132.
- [12] N.K. Myshkin, M.I. Petrokovets, A.V. Kovalev, *Tribol. Int.* 38 (2005) 910–921.
- [13] J. Karger-Kocsis, D. Felhös, D. Xu, A.K. Schlarb, *Wear* 265 (2008) 292–300.
- [14] W. Brostow, J.A. Hinze, R. Simões, *J. Mater. Res.* 19 (2004) 851–856.
- [15] W. Brostow, R. Simões, *J. Mater. Ed.* 27 (2005) 19–28.
- [16] W. Brostow, W. Chonkaew, K.P. Menard, *Mater. Res. Innovations* 10 (2006) 389–393.
- [17] K.P. Menard, *Dynamic Mechanical Analysis: A Practical Introduction*, second ed., CRC Press, Boca Raton, FL, 2008.
- [18] B.D. Beake, G.A. Bell, W. Brostow, W. Chonkaew, *Polymer Int.* 56 (2007) 773–778.
- [19] W. Brostow, W. Chonkaew, L. Rapoport, Y. Soifer, A. Verdyan, *J. Mater. Res.* 22 (2007) 2483–2487.
- [20] W. Brostow, W. Chonkaew, T. Datashvili, K.P. Menard, *J. Nanosci. Nanotechnol.* 9 (2009), in press.
- [21] F. Montefusco, R. Bongiovanni, M. Sangermano, A. Priola, A. Harden, N. Rehnberg, *Polymer* 45 (2004) 4663–4668.
- [22] M. Sangermano, R. Bongiovanni, G. Malucelli, A. Priola, A. Pollicino, A. Recca, *J. Appl. Polym. Sci.* 89 (2003) 1524–1529.
- [23] B. Bilyeu, *Characterization of cure kinetics and physical properties of a high performance, glass fiber-reinforced epoxy prepreg and a novel fluorine-modified, amine-cured commercial epoxy*. Dissertation, University of North Texas, Denton, 2003.
- [24] T.M. Chapman, K.G. Marra, *Macromolecules* 28 (1995) 2081–2085.
- [25] D.R. Lyengar, S.M. Perutz, C.A. Dai, C.K. Ober, E.J. Kramer, *Macromolecules* 29 (1996) 1229–1234.
- [26] W. Ming, M. Tian, R.D. van de Grampel, F. Melis, X. Jia, J. Loos, R. van der Linde, *Macromolecules* 35 (2002) 6920–6929.
- [27] R.R. Thomas, D.R. Anton, W.F. Graham, M.J. Darmon, B.B. Sauer, K.M. Stika, D.G. Swartzfager, *Macromolecules* 30 (1997) 2883–2890.
- [28] R.R. Thomas, D.R. Anton, W.F. Graham, M.J. Darmon, K.M. Stika, *Macromolecules* 31 (1998) 4595–4604.
- [29] R.D. van de Grampel, W. Ming, A. Gildenpennig, W.J.H. van Gennip, J. Laven, J.W. Niemantsverdriet, H.H. Brongersma, G. de With, R. van der Linde, *Langmuir* 20 (2004) 6344–6351.
- [30] J. Wang, G. Mao, C.K. Ober, E.J. Kramer, *Macromolecules* 30 (1997) 1906–1914.
- [31] S.C. Yoon, B.D. Ratner, *Macromolecules* 19 (1986) 1068–1079.
- [32] S.C. Yoon, B.D. Ratner, *Macromolecules* 21 (1988) 2401–2404.
- [33] S.C. Yoon, B.D. Ratner, B. Ivan, J.P. Kennedy, *Macromolecules* 27 (1994) 1548–1554.
- [34] S.C. Yoon, Y.K. Sung, B.D. Ratner, *Macromolecules* 23 (1990) 4351–4356.
- [35] W. Brostow, P.E. Cassidy, H.E. Hagg, M. Jaklewicz, P.E. Montemartini, *Polymer* 42 (2001) 7971–7977.
- [36] W. Brostow, B. Bujard, P.E. Cassidy, H.E. Hagg, P.E. Montemartini, *Mater. Res. Innovations* 6 (2002) 7–12.
- [37] W. Brostow, B. Bujard, P.E. Cassidy, S. Venumbaka, *Int. J. Polym. Mater.* 53 (2004) 1045–1060.
- [38] W. Brostow, P.E. Cassidy, J. Macossay, D. Pietkiewicz, S. Venumbaka, *Polym. Int.* 53 (2003) 1498–1505.
- [39] T. Kasemura, Y. Oshibe, H. Uozumi, S. Kawai, Y. Yamada, H. Ohmura, T. Yamamoto, *J. Appl. Polym. Sci.* 47 (1993) 2207–2216.
- [40] F.J. du Toit, R.D. Sanderson, W.J. Engelbrecht, J.B. Wagener, *J. Fluor. Chem.* 74 (1995) 43–48.
- [41] M. Anand, R.E. Cohen, R.F. Badour, *Polymer* 22 (1981) 361–371.
- [42] N. Inagaki, S. Tasaka, K. Mori, *J. Appl. Polym. Sci.* 43 (1991) 581–588.
- [43] M. Strobel, S. Corn, C.S. Lyons, G.A. Korba, *J. Polym. Sci. Chem.* 23 (1985) 1125–1135.
- [44] M. Strobel, P.A. Thomas, C.S. Lyons, *J. Polym. Sci. Chem.* 25 (1987) 3343–3348.
- [45] H.S. Han, K.L. Tan, E.T. Kang, *J. Appl. Polym. Sci.* 76 (2000) 296–304.
- [46] B. Bhushan, *Introduction to Tribology*, Wiley, New York, 2002.
- [47] K.P. Menard, in: W. Brostow (Ed.), *Performance of Plastics*, Hanser, Munich-Cincinnati, 2000, Chapter 8.
- [48] J.A. Marsella, W.E. Starnier, *J. Polym. Sci. Chem.* 38 (2000) 921–930.
- [49] T. Matyna, B. Gawdzik, *J. Appl. Polym. Sci.* 65 (1997) 1525–1531.
- [50] L.V. McAdams, J.A. Gannon, in: H.F. Mark (Ed.), *Encyclopedia of Polymer Science and Engineering*, vol. 6, Wiley, New York, 1985.
- [51] J.P. Pascault, H. Sautereau, J. Verdu, R.J.J. Williams, *Thermosetting Polymers*, Marcel Dekker, New York, 2002.
- [52] T.G. Fox, S. Loshaek, *J. Polym. Sci.* 15 (1955) 371–390.
- [53] W. Brostow, H.E. Hagg Lobland, M. Narkis, *J. Mater. Res.* 21 (2006) 2422–2428.
- [54] W. Brostow, H.E. Hagg Lobland, *Polym. Eng. Sci.* 48 (2008) 1982.
- [55] Y.Q. Wang, J. Li, *Mater. Sci. Eng. A* 266 (1999) 155–160.
- [56] S. Jiguet, M. Judelewicz, S. Mischler, H. Hofmann, H. Bertsch, P. Renaud, *Surf. Coat. Technol.* 201 (2006) 2289–2295.
- [57] F.P. Bowden, D. Tabor, *The Friction and Lubrication of Solids*, Clarendon Press, Oxford, 1954.
- [58] J.M. Durand, M. Vardavoulis, M. Jeandin, *Wear* 181–183 (1995) 833–839.
- [59] T.O. Larsen, T.L. Andersen, B. Thorning, M.E. Vigild, *Wear* 264 (2008) 857–868.

- [60] M.C. Romanes, N.A. D'Souza, D. Coutinho, K.J. Balkus Jr., T.W. Scharf, *Wear* 265 (2008) 88–96.
- [61] G.W. Stachowiak, A.W. Batchelor, *Engineering Tribology*, Elsevier Butterworth-Heinemann, Amsterdam, 2005.
- [62] K. Hirao, K. Watari, M.E. Brito, M. Toriyama, S. Kanzaki, *J. Am. Ceram. Soc.* 79 (2005) 2485–2488.
- [63] I.M. Hutchings, *Tribology: Friction and Wear of Engineering Materials*, Edward Arnold, 1992.
- [64] S. Bahadur, *Wear* 245 (2000) 92–99.
- [65] B. Bilyeu, W. Brostow, K.P. Menard, *J. Mater. Ed.* 19 (1999) 281–286.
- [66] B. Bilyeu, W. Brostow, K.P. Menard, *J. Mater. Ed.* 22 (2000) 107–129.
- [67] B. Bilyeu, W. Brostow, K.P. Menard, *J. Mater. Ed.* 23 (2001) 189–204.